

Measurement of ultrasonic pulse velocity with improved accuracy using automatic threshold error correction

Cite as: Rev. Sci. Instrum. 94, 045101 (2023); doi: 10.1063/5.0142739

Submitted: 16 January 2023 • Accepted: 12 March 2023 •

Published Online: 3 April 2023



View Online



Export Citation



CrossMark

Piyush,^{1,2} Nitin Dhiman,^{1,2} Bishan Kumar,^{1,2} Sanjay Yadav,^{1,2} and P. K. Dubey^{1,2,a)}

AFFILIATIONS

¹ Pressure Vacuum and Ultrasonic Metrology, CSIR National Physical Laboratory, Dr. K S Krishnan Marg, New Delhi 110012, India

² Academy of Scientific and Innovation Research (AcSIR), Ghaziabad 201002, India

^a) Author to whom correspondence should be addressed: premkduaney@gmail.com

ABSTRACT

Ultrasonic Pulse Velocity (UPV) measurement is extensively used to monitor the strength and health of concrete structures as per American Society for Testing and Materials C 597 – 09. The commercially available UPV measurement systems work on the basis of single threshold detection of the received signal. Therefore, measurement accuracy is affected due to threshold error. The effect is sensitive to the signal amplitude reaching the threshold comparator and, hence, receiver gain. It is observed that a UPV tester operating at 50 kHz to test concrete might generate an error of up to 10% in the ultrasonic transit time measurement of 50 μ s. Hence, it is of great concern and needs to be improved. In this article, the UPV measurement circuit capable of detecting and compensating the threshold error is described. The threshold error correction is achieved with the help of two threshold comparators and two hybrid counters. The circuit developed minimizes the threshold error for wide receiver gain. The measurement carried out with the developed system shows significant improvement, having deviations within 100 ns.

Published under an exclusive license by AIP Publishing. <https://doi.org/10.1063/5.0142739>

I. INTRODUCTION

Ultrasonic Pulse Velocity (UPV) is utilized for the quality assessment of rock, steel, metal alloy, limestone, marble, rubber etc.^{1–4} Of the various applications, UPV for the monitoring of health, strength, and properties of concrete structures, such as bridges and buildings, are directly linked to human safety.^{5–12} Recently, UPV has also been used to analyze the effect of reinforcement, silica fume, fiber-reinforced polymer, hybrid fiber reinforced waste liquid crystal glass sand, ground granulated blast furnace slag, crumb rubber, waste foundry sand, and crushed limestone aggregate in concrete on compressive strength of concrete.^{13–21} Therefore, accurate testing and grading of concrete for ultimate quality assurance is desired.

The UPV, in general, is measured using a direct approach due to its advantage over semi-direct and indirect methods, wherein the transmitting and receiving ultrasonic transducers are placed across the sample.²² In a UPV tester, a high-voltage pulser is used to drive the piezoelectric transducer for the generation of short duration ultrasound in the medium.²³ On the other hand, a receiving

transducer of matching frequency is used for receiving purposes. According to the American Society for Testing and Materials standard (ASTM C 597 – 09), UPV is estimated by measuring the ultrasonic time delay (transit time) in a concrete material of known path length.^{24,25} In a conventional UPV tester, a high-frequency counter is used to measure the ultrasonic transit time through the material.²⁶ The counter is triggered at the beginning of the transmitting pulse and stopped at the signal received by the receiving transducer. Concrete is a highly attenuating composite material, resulting in a low signal-to-noise ratio.²⁷ In order to precisely detect the arrival of a received signal, a threshold voltage comparator is used. The comparator produces a digital pulse at the arrival of the received signal. The threshold reference is maintained well above the ground level to avoid false triggering by the presence of electrical noise. This threshold reference becomes the source of error in the measurement of the ultrasonic transit time. It is observed that the measurement error increases with the decrease in receiver gain or with highly attenuating materials. As the UPV measurement is most widely carried out at about 50 kHz, the error due to threshold

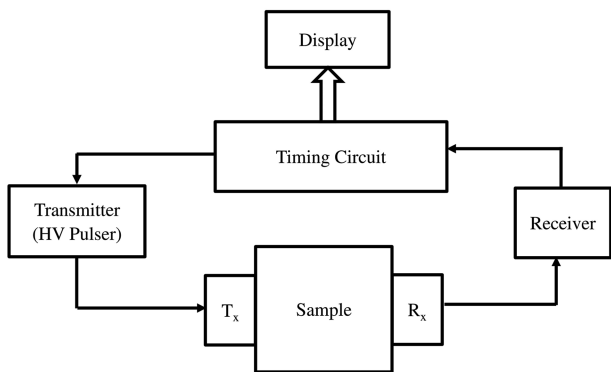


FIG. 1. The block diagram of a generalized UPV tester with the minimum required components.

selection becomes significant and might approach up to $5\ \mu\text{s}$. Therefore, an improved system, addressing the above issue, needs to be developed.

This article describes the significant error contribution of a threshold-based received signal detection used in UPV measurement. Furthermore, two thresholds and two counter based techniques, successfully developed to minimize the error caused due to the single threshold approach, are elaborated. The concept of hybrid counter has been introduced to provide the advantage of virtually running the slow counter of a microcontroller at a much higher rate for achieving better measurement resolution.^{28,29}

II. ULTRASONIC PULSE VELOCITY MEASUREMENT

A. UPV tester

The UPV tester is used to estimate the ultrasonic pulse velocity in the material by measuring the transit time through the material.³⁰

Ultrasonic transit time is the time required for the wave to travel through the material under study. The transit time can be measured with either of two techniques—through transmission and through pulse echo technique.³¹ In the pulse echo technique, a single transducer is used to produce ultrasonic waves inside the material and receive the back reflected waves by the same transducer. The merger of the transmitted and received pulses is the obvious limitation, which becomes more prominent in the 20–500 kHz that is widely used for concrete testing.³² Therefore, the through transmission method is only preferred in this frequency range. In the through transmission technique, two separate ultrasonic transducers are used—one acts as a transmitter and another one as a receiver. The UPV tester consists of three electronic blocks (transmitter, receiver, and timing), with a pair of ultrasonic transducers, to measure the ultrasonic transit time through the material, as shown in Fig. 1. The transmitter excites the transmitting transducer (Tx) with a high-voltage (600–900 V) pulse. The receiving transducer (Rx) receives the ultrasonic waves traveled through the sample. The receiver amplifies the received signal to the desired level. The amplified signal is used for transit time estimation. The time measurement is achieved in two ways—one is the counter method and another is the data acquisition method. In the data acquisition method, the complete electronic signal is acquired using a fast analog-to-digital converter. The acquired signal is used to detect the beginning of the received signal. In the counter method, the counter is stopped by a digital signal produced by a threshold comparator. The typical timing diagram of the counter method is shown in Fig. 2. The counter starts at t_s , with reference to the transmitted pulse, and stops at t_1 when the input signal crosses a fixed threshold level. Finally, the transit time is calculated by multiplying the number of counts with the clock period.

B. Error due to threshold voltage comparison

Ideally, the counter must start at the transmitted pulse and be stopped at the arrival of an ultrasonic signal at the receiving

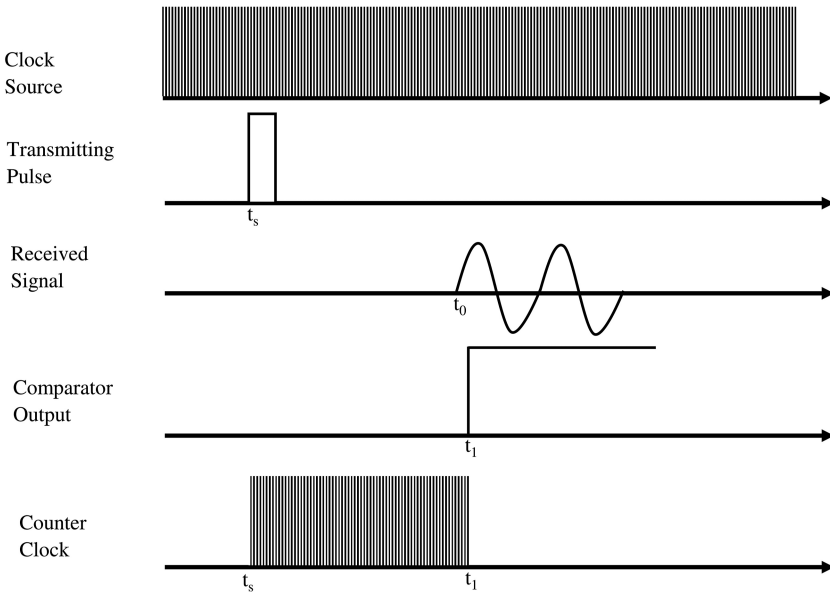


FIG. 2. Timing diagram of ultrasonic transit time measurement using the counter method.

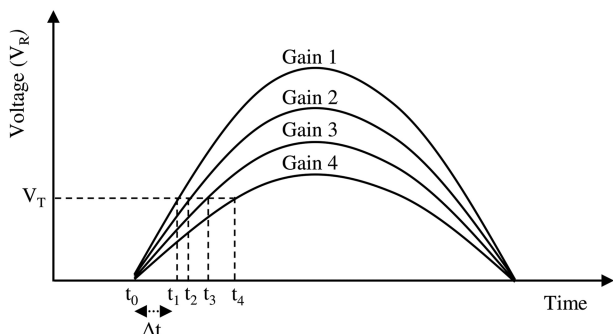


FIG. 3. Error in time measurement due to threshold amplitude as a function of the receiver signal amplitude.

transducer at instant t_0 as shown in Fig. 3. However, selecting the reference of the comparator close to zero results in a wrong trigger due to the presence of a finite noise level. So, to avoid false triggering of the counter, a certain threshold level V_T is maintained well above the electrical noise, which results in the signal arrival detection at time t_1 rather than t_0 and depends on the amplitude of the receiver output V_R . This threshold comparison adds extra time to t_0 , known as threshold error Δt . So, now Δt is given by Eq. (1).

$$\Delta t = t_1 - t_0 \quad (1)$$

$$t_1 = \frac{1}{2\pi f} \left(\sin^{-1} \left(\frac{V_T}{V_R} \right) - \Phi \right), \quad (2)$$

$$V_R = GV_s, \quad (3)$$

where, V_R is the amplitude of amplified receiver output signal. Equations (2) and (3) shows that t_1 depends on receiver gain (G), threshold level (V_T), transducer amplitude (V_s), frequency (f), and phase Φ of the received signal. Therefore, the transit time measurement by the threshold comparison approach is prone to the various above-said parameters. For instance, considering the extreme case $V_s = 1.1$ V, $V_T = 1.1$ V, $t_0 = 0$, $\Phi = 0$, and $f = 50$ kHz, and changing the gain from unity to 2500, the error Δt results in the range 1.27 ns

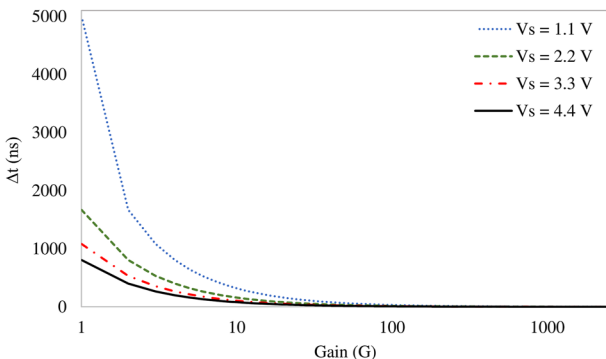


FIG. 4. The change in Δt with respect to the gain by fixing the other parameters.

to 5 μ s. Figure 4 indicates that the Δt increases with decreasing the transducer amplitude V_s and receiver gain G .

C. Threshold error estimation

As the conventional counter-based UPV testers detect the received signal by a fixed threshold amplitude comparison, in order to further study the effect of threshold on measurement, various comparator thresholds have been considered.

Now, we consider $V_R = 5$ V, $t_0 = 0$, $\Phi = 0$, and $f = 50$ kHz, and change V_T from 0 to 2500 mV to cover $\pi/6$ part of the received wave. Figure 5 shows the variation in Δt for various comparator thresholds. It is obvious from the figure that Δt changes from 0 to 1.66 μ s. In order to check the linearity of the behavior within $\pi/6$, a linear fit was applied, which shows good agreement with R-squared value of 0.9997. This linear variation can be considered, along with two threshold comparison amplitudes V_{T1} and V_{T2} , to generate another time interval $t_2 - t_1$.

Herein, if $V_{T2} = 2V_{T1}$ and $V_R > V_{T2}$, $t_1 - t_0$ can be given by Eq. (4).

$$t_1 - t_0 = t_2 - t_1. \quad (4)$$

The threshold error Δt in the measurement is now given by Eq. (5).

$$\Delta t = \frac{1}{2\pi f} \left(\sin^{-1} \left(\frac{V_{T2}}{V_R} \right) - \sin^{-1} \left(\frac{V_{T1}}{V_R} \right) \right). \quad (5)$$

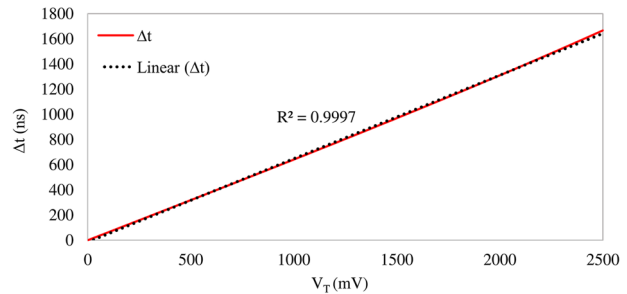


FIG. 5. The change in Δt with respect to threshold voltage V_T .

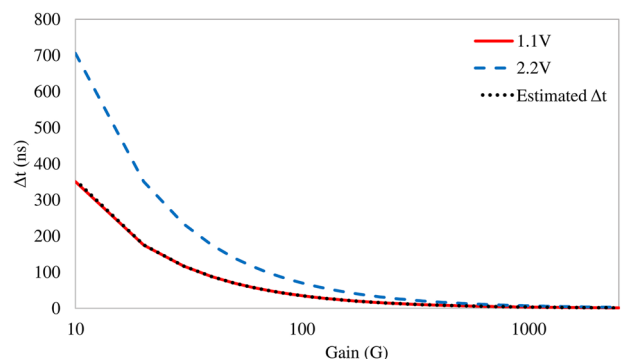


FIG. 6. The Δt at two different V_T values and estimated Δt values with respect to gain.

Thus, by implementing two threshold comparisons at voltages V_{T1} and V_{T2} , the threshold error can be estimated. Figure 6 shows the threshold error Δt at two thresholds— V_{T1} as 1.1 V and V_{T2} as 2.2 V—as a function of receiver gain G. The response in red color indicates the Δt error at 1.1 V threshold, and the response in blue shows the error at the 2.2 V threshold. A dotted black response shows that the estimated Δt error closely follows the inherent threshold error associated with V_{T1} as 1.1 V. This analogy claims to estimate the threshold error in transit time measurements.

Furthermore, to implement two threshold comparison approaches, a UPV measurement device has been developed, incorporating the two comparators and two counters.

III. EXPERIMENTAL

A. Ultrasonic pulse velocity tester with automatic threshold error correction

The developed UPV tester consists of three main stages, as shown in Fig. 7.^{28,29} The first stage is the transmitter (blue dotted box), to excite the transmitting transducer. The second stage is the receiver, for signal conditioning of the received signal from the receiving ultrasonic transducer. The last stage is the timing circuit (Red dotted box), to compute transit time. The developed UPV measurement device has a unique feature of automatic threshold error correction. A microcontroller is used to control and

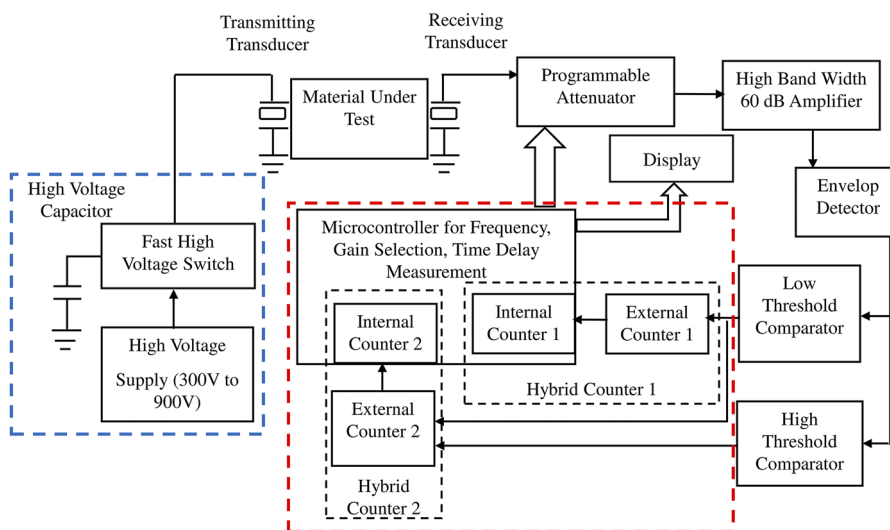


FIG. 7. Developed UPV tester with automatic threshold error correction.

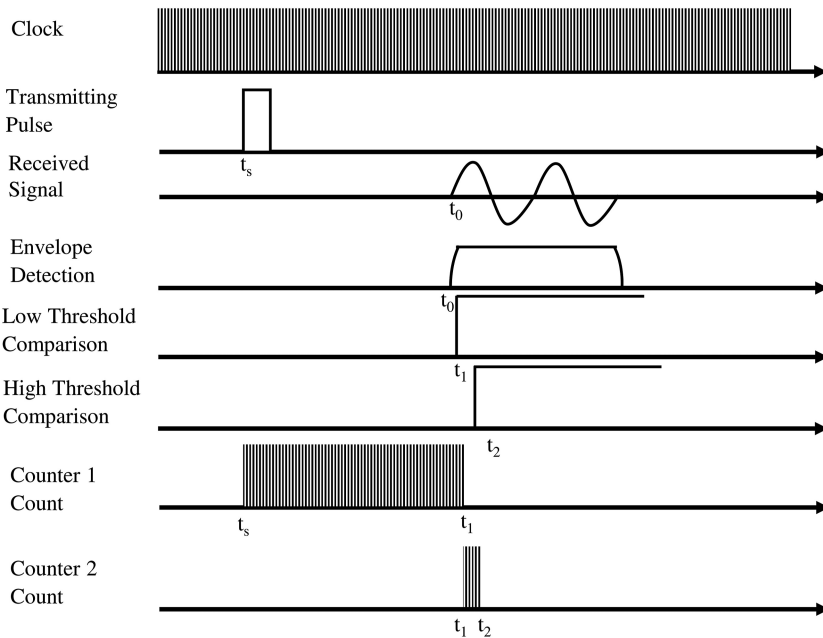


FIG. 8. The timing diagram of transit time measurement and threshold error.

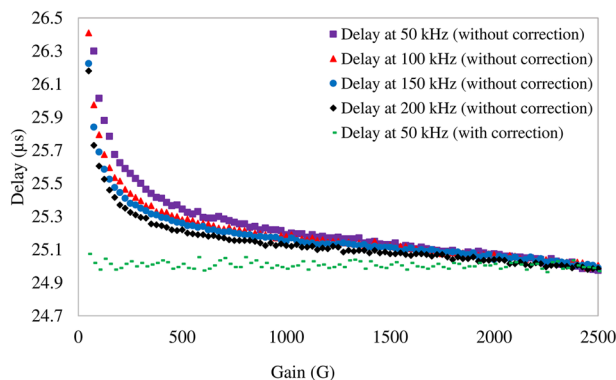


FIG. 9. Effect of receiver gain on ultrasonic transit time measurement at frequencies 50, 100, 150 and 200 kHz, along with threshold error correction at 50 kHz.

synchronize all three stages. Figure 8 depicts the timing diagram of transit time measurement with threshold error. A high-voltage capacitor is charged using high-voltage supply. The microcontroller starts counter 1 and at the same time, t_s triggers the fast high-voltage switch, to discharge the high-voltage capacitor into the transmitting transducer. The transmitting transducer produces ultrasonic waves inside the material under test. The receiving transducer receives ultrasonic waves at t_0 . The receiving transducer feeds the signal into the receiver stage. The gain of the receiver section is controlled with the help of the microcontroller by a programmable attenuator and a fixed gain amplifier. The fixed gain amplifier was chosen to maintain uniform bandwidth of 20–200 kHz throughout the gain. A sufficiently amplified signal is detected with the help of an active envelope detector. The output of the envelope detector is compared at two different voltages (V_{T1} and V_{T2}) by two comparators. The low-threshold comparator (V_{T1}) reference is maintained at 1.1 V. The high-threshold comparator (V_{T2}) is set to double of the voltage set on the low-threshold comparator, that is, 2.2 V. The low-threshold comparator stops counter 1 and, at the same time (t_1), starts counter 2. The high-threshold comparator stops counter 2 at t_2 . Counter 1 is used to count time ($t_1 - t_s$) up to the low-threshold comparison. Counter 2 is used to count the threshold time error ($\Delta t = t_1 - t_0 = t_2 - t_1$). In order to overcome the limitation of internal slow counters of the microcontroller (ATMEGA-32) and achieve

effectively high clock counting rate, additional external counters were used, as shown in Fig. 7.³³ The external counter can run much above the operating frequency of the controller, and in the present case, it was operated at 20 MHz.³⁴ The most significant part of the external counter forms the clock for microcontroller internal counters, making it hybrid with effectively large in capacity and faster counting. So, the main hybrid counter 1 is effectively 20 bit and acquires counts for time t_1 , and hybrid counter 2 is effectively 12 bit and acquires counts for error Δt . For ultrasonic transit time measurement, the microcontroller acquires data from both the hybrid counters and subtracts the excess error Δt from hybrid counter 1.

IV. RESULT AND DISCUSSION

The functionality of the developed UPV measurement device has been compared with that from the CSIR-NPL calibration facility. A reference function generator (Agilent 33250), calibrated from CSIR-NPL, was used, to provide precise time delay for the UPV device. As the threshold error measurement depends on the signal amplitude fed to the comparator, in order to study the effect of receiver gain on measurement error, a constant amplitude of 200 mV_{pp} was applied to the receiver and maintained throughout the experiment. The time delay was measured with and without threshold error correction for different gain values. Figure 9 shows the measurement performed for a 25-μs standard reference delay for receiver gain increment in steps of 25. The maximum error without threshold error correction was found to be 1.4 μs at the lowest gain value of 50. The time delay from zero to threshold of the sine wave depends on its amplitude, which ultimately also depends on the receiver gain. Therefore, it is obvious that the error reduces as the receiver gain is increased. However, the maximum deviation by the developed UPV device with threshold correction was ±50 ns even at the lower receiver gain values. This limitation is particularly due to the inherent counter resolution, which may further be improved using a faster counter clock. The standard deviation in the measurement by the threshold corrected approach throughout gain variation was found to be 0.02 μs.

It is also clear from Fig. 9 that the maximum possible error contribution due to the single threshold is limited to the transducer operating frequency. Lower the frequency, higher the chance of error contribution.

Furthermore, the functionality of the developed technique has been verified on some Perspex and concrete blocks. Table I shows

TABLE I. Effect of threshold error on ultrasonic transit time measurement on Perspex and concrete blocks.

S. No.	Sample name	Standard value assigned by NPL, India, calibration (μs)	Ultrasonic transit time, measured by the developed technique, with threshold correction (μs)	Conventional single threshold technique (μs)	Contribution of threshold error with respect to the corrected delay
1	Perspex block 1 (low)	25.76 (±0.14)	25.80	26.10	1.16% (0.3 μs)
2	Perspex block 2 (mid)	46.0 (±0.20)	45.90	46.25	0.76% (0.35 μs)
3	Perspex block 3 (high)	82.57 (±0.20)	82.65	83.20	0.66% (0.55 μs)
4	Concrete block 1	39.0 (±0.10)	39.05	40.55	3.84% (1.50 μs)
5	Concrete block 2	32.78 (±0.10)	32.65	33.30	1.98% (0.65 μs)
6	Concrete block 3	36.47 (±0.10)	36.50	37.65	3.15% (1.15 μs)

the transit time measurements carried out on Perspex blocks and concrete blocks. Three Perspex blocks have been chosen to cover the ultrasonic delay up to 100 μs .³⁵ From the table, it is evident that the concrete block 1 showed higher transit delay and highest error contribution of 3.84%, and the Perspex block 3 showed the lowest contribution error of 0.66%. The 0.66% that seems lower compared to those of the other blocks such as concrete is particularly due to the higher value of transit time in Perspex block 3, resulting in the lower percentage value. However, in the case of concrete block 1, the higher error percent is probably due to the lower amplitude of the signal received during measurement.

V. CONCLUSION

The error due to the threshold comparator becomes significant and particularly more serious when used at low receiver gain or on samples having relatively higher ultrasonic attenuation. It was observed that the error contribution reduced significantly when used with high receiver gain (above 1000). However, this may not necessarily solve the issue, particularly with high ultrasonic attenuating materials such as concrete. Therefore, the threshold error correction is required in order to estimate a more accurate ultrasonic transit time. It can also be obviously concluded that the transit time measured using the single threshold approach always gives a higher value than the actual transit time in the material, resulting in the probability of estimating the material as a lower grade material.

ACKNOWLEDGMENTS

The authors would like to thank the Director, CSIR-National Physical Laboratory, for providing the necessary facilities to carry out the above work. The author (Piyush) also thanks the University Grant Commission (UGC) New Delhi, India, for providing the research fellowships.

AUTHOR DECLARATIONS

Conflict of Interest

The authors have no conflicts to disclose.

Author Contributions

Piyush: Conceptualization (lead); Data curation (equal); Formal analysis (lead); Investigation (lead); Methodology (lead); Software (lead); Validation (lead); Visualization (equal); Writing – original draft (lead); Writing – review & editing (equal). **Nitin Dhiman:** Data curation (equal); Formal analysis (supporting); Resources (supporting); Software (supporting); Validation (supporting); Writing – review & editing (supporting). **Bishan Kumar:** Data curation (supporting); Formal analysis (supporting); Investigation (supporting); Validation (supporting); Writing – review & editing (equal). **Sanjay Yadav:** Formal analysis (equal); Funding acquisition (equal); Investigation (equal); Project administration (equal); Resources (lead); Supervision (lead); Writing – review & editing (supporting). **P. K. Dubey:** Conceptualization (lead); Data curation (supporting);

Formal analysis (supporting); Funding acquisition (lead); Investigation (equal); Methodology (equal); Project administration (lead); Resources (lead); Software (equal); Supervision (lead); Validation (lead); Visualization (equal); Writing – review & editing (lead).

DATA AVAILABILITY

The data that support the findings of this study are available from the corresponding author upon reasonable request.

REFERENCES

- ¹G. Trtnik, F. Kavčič, and G. Turk, “Prediction of concrete strength using ultrasonic pulse velocity and artificial neural networks,” *Ultrasonics* **49**, 53–60 (2009).
- ²E. Hu and W. Wang, *Math. Probl. Eng.* **2016**, 6762076 (2016).
- ³E. Vasanello *et al.*, *Ultrasonics* **60**, 33–40 (2015).
- ⁴Y. Mahmutoglu, *Environ. Earth Sci.* **76**(12), 1–20 (2017).
- ⁵F. Saint-Pierre *et al.*, *Constr. Build. Mater.* **125**, 1022–1027 (2016).
- ⁶A. B. Espinosa *et al.*, *Appl. Sci.* **13**(2), 874 (2023).
- ⁷Y. Boussahoua *et al.*, *Asian J. Civ. Eng.* **42**, 1–15 (2023).
- ⁸T. Zhou *et al.*, *J. Build. Eng.* **68**, 106121 (2023).
- ⁹Y. Lin, C.-P. Lai, and T. Yen, *Mater. J.* **100**(1), 21–28 (2003).
- ¹⁰U. Dilek, *J. Perform. Constr. Facil.* **21**(5), 337–344 (2007).
- ¹¹G. Karaiskos *et al.*, *Smart Mater. Struct.* **24**(11), 113001 (2015).
- ¹²T. Yilmaz and B. Ercikdi, *Nondestr. Test. Eval.* **31**(3), 247–266 (2016).
- ¹³N. Fodil, M. Chemrouk, and A. Ammar, *Eur. J. Environ. Civ. Eng.* **25**(2), 281–301 (2021).
- ¹⁴G. Hong *et al.*, *Materials* **14**(10), 2476 (2021).
- ¹⁵A. Mirmiran and Y. Wei, *J. Eng. Mech.* **127**(2), 126–135 (2001).
- ¹⁶A. S. Nik and O. L. Omran, *Constr. Build. Mater.* **44**, 654–662 (2013).
- ¹⁷C.-C. Wang and H.-Y. Wang, *Constr. Build. Mater.* **137**, 345–353 (2017).
- ¹⁸M. Shariq, J. Prasad, and A. Masood, *Constr. Build. Mater.* **40**, 944–950 (2013).
- ¹⁹B. S. Mohammed, N. J. Azmi, and M. Abdullahi, *Constr. Build. Mater.* **25**(3), 1388–1397 (2011).
- ²⁰G. Singh and R. Siddique, *Constr. Build. Mater.* **26**(1), 416–422 (2012).
- ²¹R. Solis-Carcaño and I. Eric Moreno, *Constr. Build. Mater.* **22**(6), 1225–1231 (2008).
- ²²P. Turgut and O. F. Kucuk, *Russ. J. Nondestr. Test.* **42**(11), 745–751 (2006).
- ²³R. Ghosh *et al.*, *J. Build. Eng.* **16**, 39–44 (2018).
- ²⁴American Society for Testing and Materials C597, 2009.
- ²⁵K. Komlos *et al.*, *Cem. Concr. Compos.* **18**(5), 357–364 (1996).
- ²⁶K. i. Kondo *et al.*, *J. Acoust. Soc. Am.* **58**(4), 928–929 (1975).
- ²⁷P. Anugonda, J. S. Wiehn, and J. A. Turner, *Ultrasonics* **39**(6), 429–435 (2001).
- ²⁸P. K. Dubey, S. Yadav, and Piyush, Indian Patent File No. 202111048097 (21 October 2021).
- ²⁹P. K. Dubey, S. Yadav, and Piyush, U.S. Patent Application Reference No. 17/936018 (28 October 2022).
- ³⁰R. E. Thill and T. R. Bur, *Geophysics* **34**(1), 101–105 (1969).
- ³¹H. Jain, E. G. Tarpara, and V. H. Patankar, *Rev. Sci. Instrum.* **91**(9), 094704 (2020).
- ³²S. Rajagopalan, S. J. Sharma, and P. K. Dubey, *Rev. Sci. Instrum.* **78**(8), 085104 (2007).
- ³³See <http://ww1.microchip.com/downloads/en/DeviceDoc/doc2503.pdf> for ATmega32 datasheet.
- ³⁴See https://doc.platan.ru/pdf/datasheets/nxp/74HC_HCT393_3-38357.pdf for 74HC393 datasheet.
- ³⁵Indian Standard 516 (Part 5/Sec 1), 2018.